Transition from linear Landau damping to nonlinear Bernstein-Greene-Kruskal modes via phase synchronization

Shaokang Xu,[1] Z. B. Guo,[1,*] and Ö. D. Gürcan[2,†]

[1]*State Key Laboratory of Nuclear Physics and Technology, School of Physics, Peking University, Beijing 100871, China*

[2]*Laboratoire de Physique des Plasmas, CNRS, Ecole Polytechnique, Sorbonne Université, Université Paris-Saclay, Observatoire de Paris, F-91120 Palaiseau, France*

(Received 20 October 2020; accepted 26 January 2021; published 15 February 2021)

Dynamics of the transition from a linear plasma wave to a nonlinear state characterized by the Bernstein-Greene-Kruskal mode is studied within the framework of the Vlasov-Poisson system. In the linear stage, the plasma distribution function (f) develops finer and finer structures in velocity space through a series of "mixing" processes leading to the Landau damping of the plasma wave. These mixing processes inevitably result in strong phase irregularities in velocity space. Using numerical simulations, it was observed that starting from the wave-particle resonance region, this irregular phase pattern gets "smoothed out" through a process of spreading of phase synchronization, which tends to reduce Landau damping, facilitating the formation of the nonlinear plasma wave as a fully synchronized final state. It is also found that there exists a residual damping for the quasisteady nonlinear wave when the phases of the particles are not fully synchronized.

DOI: 10.1103/PhysRevE.103.023208

I. INTRODUCTION

The concept of*Landau damping* as the collisionless damping of a perturbed Maxwellian plasma through wave particle interactions [1] is one of the pillars of plasma physics studies since its key mechanisms were verified repeatedly in experiments (e.g., Ref. [2]) and observed in countless numerical simulations [3–5] of different kinds of plasmas. The phenomenon generalizes readily to a system of coupled oscillators [6] and is probably one of the key contributions of plasma physics to science at large [7] as it is observed in many other physical problems.

Even though Landau damping is a well established robust phenomenon, it is also well known in the plasma physics community that if the system is initially excited by a strong perturbation, the nonlinear interaction induced particle trapping effect [8–10] can lead to saturation, resulting in the formation of the Bernstein-Greene-Kruskal (BGK) mode [11–13]. The history of its study probably goes back to the first calculation of the nonlinear Landau damping rate by O'Neil for an electron plasma wave with constant and uniform amplitude [14]. The general issue of the nonlinear dynamics of Landau damping attracted significant attention throughout the years as it is pertinent to key questions in different areas of plasma physics. For instance, the case of an arbitrarily varying amplitude of a laser driven electron plasma wave has been analyzed for stimulated Raman scattering in the context of inertial confinement fusion [15]. The subject even attracted detailed mathematical scrutiny as Mouhot and Villani studied the nonlinear Landau damping from a mathematical perspective, based on the assumption of regularity of its solutions [7,16]. It is also interesting to note from the point of view of coupled oscillators that Landau damping takes place below a certain threshold of synchronization [6], implying that above such a threshold evolution towards a nonlinearly synchronized state (corresponding to the BGK mode in the plasma context) is preferred. This suggests that synchronization or its absence must also be a key issue for Landau damping in plasma physics.

Thus, in this article, we approach the problem of nonlinear Landau damping from the perspective of *phase synchronization* dynamics [17] by considering the nonlinear behavior of a plasma wave that is self-generated by a large initial perturbation (without any external drive, such as a laser beam, for example). This underlines a fundamental difference to previous works that study nonlinear Landau damping [7,14–16]. In particular, we focus on the evolution of the phase pattern of the particle distribution function in velocity space, which is shown to be a powerful tool in the study of nonlinear plasma waves. Although there are multiple examples of global wave phases playing an important role in the nonlinear dynamics of plasma physics, such as, for example, the study of the role of global phases in strong coupling Brillouin scattering [18,19], the phase dynamics of the particle distribution function in velocity space, which contains detailed information on wave-particle resonant interaction is rarely studied in detail.

Based on the phase pattern of the electron distribution function in velocity space, we find that there exists a third state between the linear and the nonlinear Landau damping, which we call the transition stage in this paper. The transition stage is crucial in order to understand the depletion of the linear Landau damping and the formation of the nonlinear wave. In terms of phase dynamics, these three stages correspond, respectively, to *phase mixing*, *phase synchronization*

*guozhipku@gmail.com

†ozgur.gurcan@lpp.polytechnique.fr

spreading, and *full phase synchronization* of the electron distribution function in velocity space. Furthermore, the damping rate is different in these three periods: In the linear stage the plasma wave damps as $e^{-\gamma t}$, in the transition stage the plasma wave damps algebraically following $t^{-\beta}$, and in the fully nonlinear stage no evident damping is observed. It is interesting to observe that in the transition stage, the phase mixing and phase synchronization coexist, which forms a chimera phase pattern [20] in velocity space. The rate of spreading of the synchronization of the phases determine how fast the depletion of the damping occur, resulting either in a quick or a slow decrease of the damping rate. In some marginal cases, depending on initial conditions, the damping may persist indefinitely as there appears to be no significant spreading of the phase synchronization even as time tends to infinity.

In order to formulate an analytical description of these phenomena, we employ the method used by Strogatz *et al.* [6] and Kuramoto [21] to study the synchronization of coupled oscillators and treat the nonlinear wave-particle interaction term as a complex order parameter [22]. This formulation can help understand the nonlinear wave-particle interaction inherent in the numerical simulation. We find, in particular, that the primary physical mechanism of phase synchronization in this system is the synchronization of individual electron motions as they accelerate or decelerate due to their relative phase with the wave, which, in turn, is collectively generated by the motions of all the other electrons.

This paper is organized as follows: In Sec. II the phase and amplitude equation of the electric field and the particle distribution function is derived from the Vlasov-Poisson equation. The phase mixing and the phase synchronization spreading in the transition stage is discussed in Sec. III. The self-regulation regime of the kinetic and electric energy flow in fully synchronized stage is studied in Sec. IV. In the end the main results of this article are summarized, and some possible applications to more complicated systems are proposed.

II. PHASE EQUATIONS OF THE VLASOV-POISSON SYSTEM

The fundamental model of a kinetic plasma is the Vlasov-Poisson equation, written as

$$\begin{aligned} \frac{\partial f}{\partial t} + v\frac{\partial f}{\partial x} - E\frac{\partial f}{\partial v} &= 0, \\ \frac{\partial E}{\partial x} &= 1 - \int_{-\infty}^{+\infty} f\, dv, \end{aligned} \tag{1}$$

where $f(x, v, t)$ is the electron distribution function and $E(x, t)$ is the electric field. Here (x, v) is the two dimensional phase space with one dimension (1D) in space x and 1D in velocity v. The ions are considered as a uniform motionless background in contrast to the high frequency Langmuir oscillations of electrons. Equation (1) is in dimensionless form with the space coordinate x normalized by the Debye length λ_D, the time t normalized by the inverse plasma frequency ω_{pe}^{-1}, and the velocity v normalized by the electron thermal velocity v_{Te}. The boundary is assumed to be periodic in the x direction for simplicity. This means that the results that are presented here are rigorously valid only for a spatially periodic system or one that can be modeled as such. However, note that choosing a compact initial perturbation far from the boundaries, a similar exercise can be performed to imitate an infinite system. This allows us to write this system in Fourier space as

$$\begin{aligned} \frac{\partial f(k, v, t)}{\partial t} &= -ikvf(k, v, t) + \left(E(x, t)\frac{\partial f(x, v, t)}{\partial v}\right)_k, \\ ikE(k, t) &= \delta(k) - \int_{-\infty}^{+\infty} f(k, v, t)dv, \end{aligned} \tag{2}$$

where $f(k, v, t)$ and $E(k, t)$ are the spatial Fourier transforms of the distribution function and the electric field, respectively. The term $[E(x, t)\partial_v f(x, v, t)]_k$ is the Fourier transform—which can be computed using a fast Fourier transform algorithm in numerical applications—of the nonlinear term representing the wave-particle interaction contribution to the mode k. Here, $\delta(k)$ is the Dirac δ function representing the Fourier transform of the ion distribution function. Due to the quasineutrality condition, the mean-field $E(k = 0)$ is zero, which means $\int_{-\infty}^{+\infty} f_0(v, t)dv = 1$, hence, the total number of particles is conserved.

We introduce a complex order parameter $\mathcal{R}(k, v, t)$ as

$$\mathcal{R}(k, v, t) \equiv \left(E(x, t)\frac{\partial f(x, v, t)}{\partial v}\right)_k, \tag{3}$$

with which Eq. (2) can be written as

$$\frac{\partial f}{\partial t} = -ikvf + \mathrm{Re}^{i\Theta}, \tag{4}$$

where $R(k, v, t)$ and $\Theta(k, v, t)$ are the amplitude and the phase of the complex order parameter, respectively.

The distribution function in Fourier space $f(k, v, t)$ can be characterized by its phase $\theta_f(k, v, t)$ and amplitude $|f(k, v, t)|$: $f(k, v, t) \equiv |f(k, v, t)|e^{i\theta_f(k,v,t)}$, whose evolution can be obtained by inserting these into (4) as

$$\frac{\partial |f_k|}{\partial t} = R_k \cos(\Theta_k - \theta_f), \tag{5}$$

$$\frac{\partial \theta_f}{\partial t} = -kv + \frac{R_k}{|f_k|}\sin(\Theta_k - \theta_f). \tag{6}$$

Note that Eq. (6) is similar to the mean-field equation of the Kuramoto model [22,23], which was initially developed by Kuramoto to study the synchronization of coupled oscillators. In contrast to Eq. (6), the Kuramoto model is written as

$$\partial\theta_n/\partial t = \omega_n + Kr\sin(\psi - \theta_n), \tag{7}$$

with $n = 0, \ldots, N$ being the oscillator number. The nonlinear interaction among the oscillators is given by the term $Kr\sin(\psi - \theta_n)$, where K is a constant defining the coupling strength, r is an evolving real variable between 0 and 1 measuring the coherence of the system (the larger the r, the more coherent the system becomes), and ψ is an evolving mean phase created by all the oscillators. Using the coupling to the mean phase instead of the direct couplings between each two oscillators, the Kuramoto model allows us to cut an all-to-all coupling problem into two separated steps: An all-to-one coupling followed by a one-to-all coupling. First, all the oscillators create a time evolving mean phase, which can be resolved by the self-consistent relation:

TABLE I. Comparison of the phase equation in Kuramoto and Vlasov systems.

	Kuramoto	Vlasov
Phase equation	$\frac{\partial\theta_n}{\partial t} = \omega_n + Kr\sin(\psi - \theta_n)$	$\frac{\partial\theta_f}{\partial t} = -kv + \frac{R_k}{\lvert f_k\rvert}\sin(\Theta_k - \theta_f)$
Natural frequency	ω_n	$-kv$
Nonlinear coupling	$Kr\sin(\psi - \theta_n)$	$\frac{1}{\lvert f_k\rvert}R_k\sin(\Theta_k - \theta_f)$
Coupling strength	K	$\frac{1}{\lvert f_k\rvert}$
Self-consistency	$re^{i\psi} = \frac{1}{N}\sum_n e^{i\theta_n}$	$R_k e^{i\Theta_k} = [E(x,t)\frac{\partial f(x,v,t)}{\partial v}]_k$

$re^{i\psi} = \frac{1}{N}\sum_n e^{i\theta_n}$. Then each oscillator interacts exclusively with this mean phase resulting in a nonlinear coupling of the form $Kr\sin(\psi - \theta_n)$.

Table I compares the Vlasov and the Kuramoto systems. The wave-number/velocity pair k, v in Vlasov corresponds to the oscillator number n in Kuramoto, and the natural frequency ω_n in Kuramoto is represented by $-kv$ in Vlasov. Therefore, the phase of the distribution function as a function of scale $\theta_f(k, v)$ in Vlasov corresponds to the phase of the oscillator θ_n in Kuramoto, and the complex order parameter $R(k, v, t)e^{i\Theta(k,v,t)}$ represents the phase coherence variable $re^{i\psi}$, which defines the nonlinearity of the mode k and allows a separation of the problem into two conceptual steps as described above for the Kuramoto system. Note that the transformation of the Kuramoto model into a mean-field model as discussed above is a simple theoretical transformation where the coherence variable r, the mean phase ψ, and the coupling strength K can be chosen as constants for all oscillators. But the Vlasov equation describes a more complex physical system where the nonlinear term and its phase and amplitude depend on the wave number and velocity.

More generally, the phase equations of the Vlasov and Kuramoto systems, [i.e., Eqs. (6) and (7)] both have the form of an Adler equation [24] with kv as the free streaming frequency and $R_k/|f_k|$, the phase coupling coefficient that locks θ_f to the mean phase Θ_k (or θ_E since as we will show later, the two are strongly correlated).

Note that for the Vlasov system, the Poisson equation plays the role of the self-consistency relation that is used to close the system in the Kuramoto model. In order to write the Poisson equation in this form, we recall that the electric field in Fourier space is defined as: $E(k) \equiv |E(k)|e^{i\theta_E(k)}$ with $|E(k)|$ and $\theta_E(k)$, the amplitude and the phase of $E(k)$. Substituting this into Eq. (2) we obtain the evolution equations for $|E(k)|$ and $\theta_E(k)$ as

$$\frac{\partial|E(k)|}{\partial t} = \int_{-\infty}^{+\infty} v|f|\cos(\theta_f - \theta_E)dv, \tag{8}$$

$$\frac{\partial\theta_E(k)}{\partial t} = \frac{1}{|E|}\int_{-\infty}^{+\infty} v|f|\sin(\theta_f - \theta_E)dv. \tag{9}$$

III. PHASE SYNCHRONIZATION SPREADING IN THE TRANSITION STAGE

The Vlasov-Poisson system described above can be implemented numerically in the (x, v) plane using a second order Euler method [5]. The phase space (x, v) is discretized in a rectangular domain $D \equiv \{(x, v)|0 \leqslant x < L_x,\ |v| \leqslant v_{\max}\}$ with $L_x = 4\pi$, the periodic spatial length and $v_{\max} = 6$, the cutoff velocity. The space x and the velocity v are discretized with a homogeneous mesh size $\delta x = L_x/N_x$ and $\delta v = 2v_{\max}/N_v$, where $N_x = 256$ and $N_v = 256$ are the number of grid elements along the x and v directions, respectively. The wave number in Fourier space is defined as $k_n = \frac{2\pi n}{L_x}$ with $n = 0, \ldots, \frac{N_x}{2}$. Such an implementation can be used to simulate the long time behavior of a perturbed Maxwellian plasma by using the following initial condition:

$$f(x, v, t = 0) = \frac{1}{\sqrt{2\pi}}\exp\left(-\frac{v^2}{2}\right)[1 + \alpha\cos(kx)], \tag{10}$$

where $\alpha = 0.15$ determines the initial perturbation strength and $k = 0.5$ is the initial excitation wave number, which corresponds to the first Fourier mode (i.e., the largest scale) available in the wave-number domain.

A. Free streaming: phase mixing

Here we focus on the evolution of the large scale mode (k_1). $|E(k_1, t)|$ as a function of time $t = [0, 8000\omega_{pe}^{-1}]$ is presented in Fig. 1 with a long enough integration time so that the spectrum contains all the different states of $|E(k_1)|$. For $t \lesssim 20\omega_{pe}^{-1}$, $|E(k_1, t)|$ damps exponentially due to linear Landau damping. The analytical damping rate [25] for this case is as follows: $\gamma(k_1 = 0.5) = -0.1536$. The numerical implementation can reproduce the analytical result well since it agrees with the analytical prediction as shown in the subplot of Fig. 1. After the linear stage, the wave damps algebraically

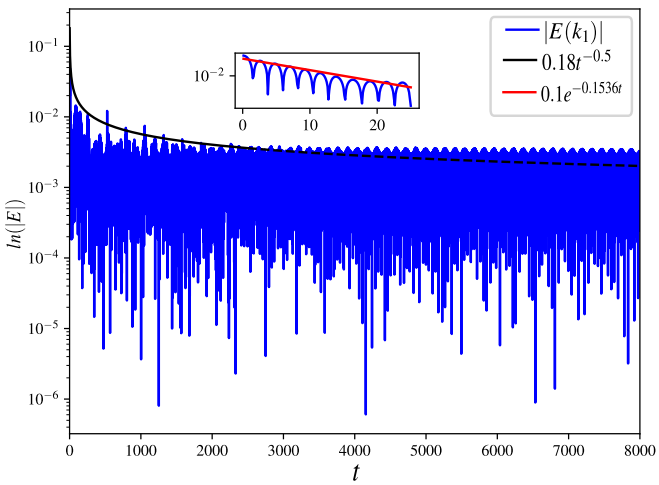

FIG. 1. The evolution of $|E(k_1)|$ in the simulation of $\alpha = 0.15$. The subplot compares $|E(k_1, t < 20\omega_{pe}^{-1})|$ (blue) to $0.1e^{-\gamma t}$ (red line) with $\gamma = 0.1536$. The black line show $t^{-\beta}$ with $\beta = -0.5$. $|E(k_1, t < 2500\omega_{pe}^{-1})|$ can be fit with $0.12t^{-0.5}$ (the black solid line). For $t > 2500\omega_{pe}^{-1}$, $t^{-\beta}$ (black dashed line) is no longer valid.

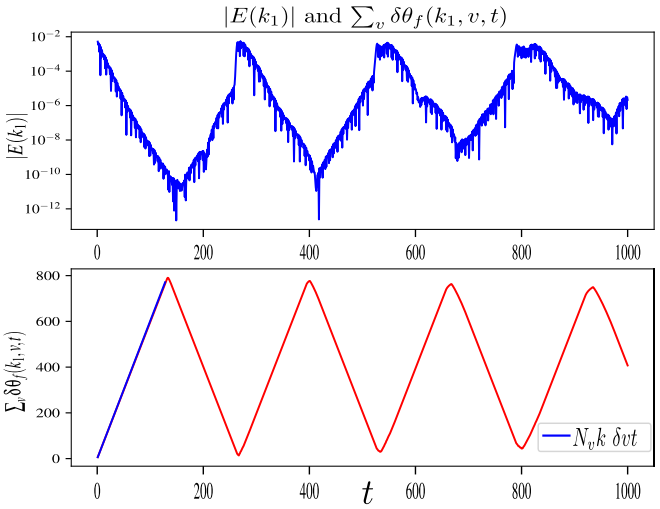

FIG. 2. Correlation of $|E_k|$ and $\sum_v \delta\theta_f(k_1, v)$ in the simulation of $\alpha = 0.01$.

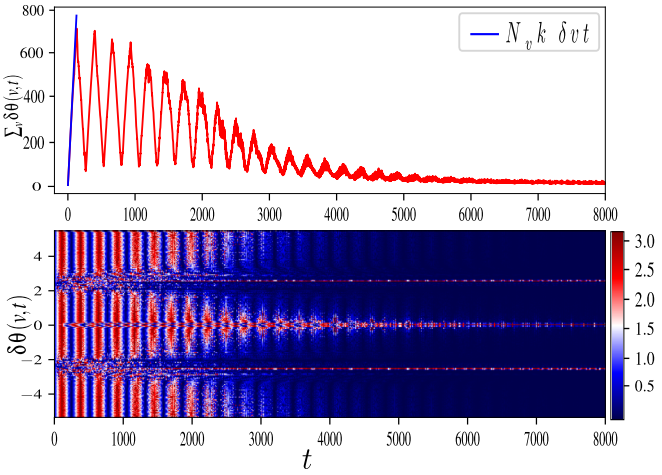

FIG. 3. The sum of phase difference $\sum_v \delta\theta_f(k_1, v, t)$ (top) and the detailed structure of the phase difference $\delta\theta_f(k_1, v, t)$ in velocity space for $t = [0, 8000\omega_{pe}^{-1}]$.

in the form $t^{-\beta}$ (black line), with $\beta = 0.5$ up to $t \approx 2500\omega_{pe}^{-1}$. After that, it is hard to observe any damping of the wave.

In previous studies [26], the linear Landau damping arises from the phase mixing of the particle distribution function in velocity space. This can be explained using the Poisson equation: $ik|E_k|e^{i\theta_E} = -\int_{-\infty}^{+\infty} |f_k(v)e^{i\theta_f} dv$. In the phase-slip state, θ_f's are randomly distributed in velocity space, and the integral gives a small $|E_k|$. On the other hand, in the phase-locked state, θ_f's are organized into patches in velocity space, and the integral is likely to give a finite value for $|E_k|$ [27]. In numerical simulations, the phase mixing can be measured quantitatively by the sum of the phase differences between neighboring velocity points, which can be defined as follows:

$$\sum_v \delta\theta_f(k, v) = \sum_j \min\{[\theta_f(k, v_{j+1}) - \theta_f(k, v_j)] \mathrm{mod}\, 2\pi \times [\theta_f(k, v_j) - \theta_f(k, v_{j+1})] \mathrm{mod}\, 2\pi\}.$$

If $\sum_v \delta\theta_f(k, v)$ is large (small), $\theta_f(k, v)$ is disorganized (organized), and the phase mixing is strong (weak) in velocity space, resulting in a decrease (growth) in $|E_k|$. This can be observed in numerical simulations as shown in Fig. 2.

In Eq. (6), the free streaming frequency represents the natural frequency for the electron distribution function with the wave-number k and velocity v. Since this is a function of the velocity, it leads to phase slipping in velocity space. In contrast, the wave-particle interaction acts as a phase coupling force locks θ_f to the mean phase. If we assume that the dynamics for that wave number is dominated by free streaming, i.e., $R_k/|f_k| \ll kv$, the solution is $f(k, v, t) = f(k, v, 0)e^{-ikvt}$. In this case, $\theta_f(k, v)$ and $\delta\theta_f(k, v)$ are given as follows:

$$\theta_f(k, v, t) = -kvt + \theta_f(k, v, 0),$$
$$\delta\theta_f(k, v, t) = k\,\delta v\, t + \delta\theta_f(k, v, 0).$$

This means that the sum of the phase difference becomes: $\sum_v \delta\theta_f(k, v, t) = N_v k\,\delta v\, t$, resulting in a periodic evolution with the period $T = \frac{2\pi}{k\,\delta v}$ [5,28]. For timescales that are much shorter than T, such as that of the linear Landau damping, the free streaming frequency causes $\sum_v \delta\theta_f(k, v, t)$ to increase linearly in time, which results in the phase mixing and the damping of the plasma wave. Note that in this case the system is able to go back to its initial state at $t = nT$ with n, an integer because $f(k, v, t) = f(k, v, 0)e^{-ikvt}$. This agrees approximately with the frequency observed in the linear stage. In the bottom of Fig. 2, $\sum_v \delta\theta_f(k_1, v, t)$ oscillates with a period $T \simeq 266.78\omega_{pe}^{-1}$, which is close to the analytical result of $T = \frac{2\pi N_v}{2k_1 v_{\max}} = 267.03\omega_{pe}^{-1}$. The growth of $\sum_v \delta\theta_f(k_1, v, t)$ can be fit with $N_v k\,\delta v\, t$ (blue), hence, at this stage the nonlinearity is negligible.

However, the system cannot go back exactly to its initial state because the maximum of $|E(k_1, t)|$ decreases slowly in time with the timescale T as shown in Figs. 1 and 2. This suggests the existence of another type of damping in the system. Furthermore, this new damping is different from the linear Landau damping for two reasons: First, the timescale of the linear Landau damping is on the order of $\frac{2\pi}{k_1 v_{ph}}$ with v_{ph}, the phase velocity of the electric wave, but the timescale of this new damping is on the order of $T = \frac{2\pi}{k_1\,\delta v}$ and $T \gg \frac{2\pi}{k_1 v_{ph}}$; second, linear Landau damping ($e^{-\gamma t}$) is much stronger than this new damping ($t^{-\beta}$).

Note that the decrease in the maximum perturbed wave amplitude is comparable to that observed in the resonance absorption of a nonlinear electron plasma wave in a laser plasma system [29,30] where the maximum of the perturbed electric field and electron density decease periodically in space before the wave breaking. However, these works focus on the threshold of laser intensity in the plasma wave breaking whereas we study the details of this decrease.

B. Transition stage: chimera phase pattern

Since we observe another damping after the linear stage, it would be interesting to explore the details of its nature. The sum of the phase differences presented in Fig. 3 shows that $\sum_v \delta\theta_f(k_1, v, t)$ is still very large in this stage, even though its maximum decreases slowly in time. This

means that although the main mechanism still is phase mixing, its efficacy decreases over time.

In Eq. (6), the nonlinear wave-particle interaction is the only factor that can counter the effect of phase mixing due to free streaming. Since $R_k/|f_k|$ depends on velocity, this balance for $\theta_f(k_1, v)$ will be velocity dependent, which may result in an inhomogeneous phase pattern in velocity space. As the phase is still disorganized, but the sum of the phase difference decreases, evolution of the phase difference seems to be a more important variable in comparison to the phase itself. $\sum_v \delta\theta_f(k_1, v, t)$ and $\delta\theta_f(k_1, v, t)$ are presented, respectively, at the top and the bottom plots of Fig. 3. In the wave-particle resonance region, i.e., v close to $v_{ph} = 2.83$ [28], $\delta\theta_f$ is strongly modified by the wave-particle resonance and becomes zero before the rest of the phase space as the system evolves. Note that phase differences being close to zero is a direct result of the synchronization of those phases. However, in the rest of the velocity space, phase difference keeps evolving periodically between $-\pi$ and π, suggesting that these regions of the velocity space are still dominated by free streaming. As the time passes, the phase synchronization spreads from the resonance region to the rest of the velocity space, resulting in a significant decrease in $\sum_v \delta\theta_f(k_1, v, t)$ and, thus, to suppression of phase mixing in velocity space.

The structure of the phase difference indicates that $\theta_f(k_1, v, t)$ is partially synchronized in velocity space during the phase synchronization spreading. In the region where $\theta_f(k_1, v, t)$ is not yet synchronized, the particle motion is dominated by free streaming. During this stage linear and nonlinear effects coexist and dominate in different regions of the velocity space. We call this the *transition stage* since it corresponds to the transition from the linear to the fully nonlinear stage.

The plasma wave is collectively generated by the streaming motion of electrons with different velocities, and the frequency ω_k of this wave is actually an average frequency over those different velocities. If electrons in different velocities manage to beat together with this average frequency, synchronization occurs. Since the natural frequencies of those electrons that are traveling with a velocity close to v_{ph}, are close to the plasma wave frequency, they can synchronize with the plasma wave frequency very easily. On the other hand, the electrons that are either very fast or very slow, (i.e., $v \gg v_{ph}$ or $v \ll v_{ph}$), the nonlinear term $\frac{R(k)}{|f(k)|}\sin(\Theta - \theta_f)$ needs to make up for the difference between their natural frequency and the frequency of the plasma wave. In order to satisfy this, $R(k_1, v)/|f(k_1, v)|$ should be, at least, on the order of $k|v - v_{ph}|$ since $|\sin(\Theta - \theta_f)| \leqslant 1$. The fact that $R(k_1, v)/|f(k_1, v)|$ should be on the order of $k|v - v_{ph}|$ for phase synchronization, indicates that it is easier to synchronize if v is closer to v_{ph}. Thus, it is observed that the phase synchronization occurs initially in wave-particle resonance region and then spread to other regions.

Since $|f(k_1, v)|$ is large and the nonlinearity is weak in the linear stage, $R(k_1, v)/|f(k_1, v)|$ is small compared to the free streaming frequency and, therefore, the k_1 mode undergoes phase mixing, resulting in decreasing of $|E(k_1)|$ and $|f(k_1, v)|$. This, in turn, causes $R(k_1, v)/|f(k_1, v)|$ to grow in time until the synchronization of the phases since $|E(k_1)|$

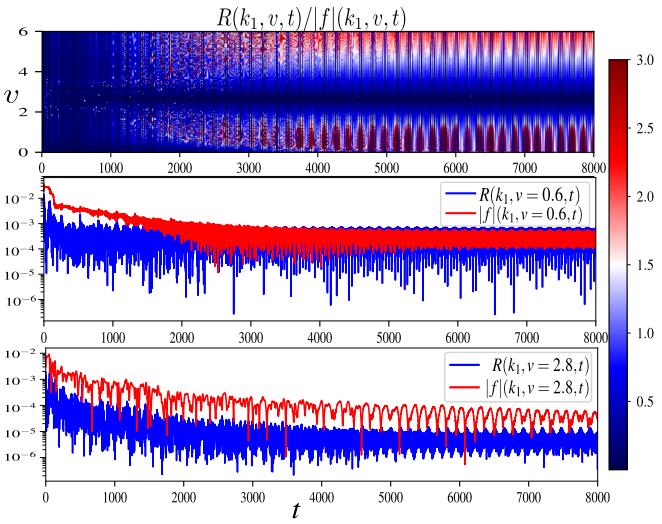

FIG. 4. $|R(k_1, v)|/|f(k_1, v)|$ (top) as a function of time. The second and the third figures present $|R(k_1, v, t)|$ (blue) and $|f(k_1, v, t)|$ (red) for $v = 0.6$ and $v = 2.8$, respectively.

and $|f(k_1, v)|$ keep decreasing as long as the phase mixing continues. When $R(k_1, v)/|f(k_1, v)|$ is on the order of $k|v - v_{ph}|$, $\partial_t\theta_f(k_1, v)$ matches the frequency of the plasma wave, and the saturation occurs.

The dynamics of $R(k_1, v)/|f(k_1, v)|$ is depicted in Fig. 4. In the resonance region $R(k_1)/|f(k_1)|$ is close to zero because $R(k_1, v \sim v_{ph})$ is much smaller than $|f(k_1, v \sim v_{ph})|$ during the whole simulation as shown in the bottom of Fig. 4. This is due to the fact that resonant electrons see a stationary wave [9] since $v \sim v_{ph}$. Thus, the plasma wave pushes these electrons to neighboring regions causing a flattening of the distribution function (i.e., making $\partial_v f \sim 0$) in the resonance region. Since $\mathcal{R} \propto \partial_v f$, the strength of nonlinearity ends up being small in the resonance region. The fact that $R(k_1, v \sim v_{ph})/|f(k_1, v \sim v_{ph})|$ remains close to zero means that the natural frequency of the resonant electrons match the frequency of the plasma wave. For the faster and slower electrons, $R(k_1)/|f(k_1)|$ keeps growing in the transition stage due to damping of $|f(k_1, v)|$ in the phase mixing regime. In the end the nonlinear phase coupling modifies the natural frequency of these electrons sufficiently to allow them to synchronize themselves to the plasma wave.

Complete phase synchronization in velocity space requires a large value of $R(k_1)/|f(k_1)|$, which is also similar to what happens in the Kuramoto model. In Kuramoto, the global synchronization among oscillators can be achieved if the coupling strength, which is a global quantity independent of the oscillator number, is larger than a critical value, and the global synchronization is independent of the initial phase distribution [22]. In Vlasov, on the other hand, the phase and the amplitude are strongly coupled, which is a significant distinction from the Kuramoto model. In particular, there is a feedback mechanism in the Vlasov system since phase mixing causes $|f(k_1)|$ to decrease, which, in turn, increases the effect of phase locking.

In order to estimate the damping parameter β that we observe in the transition stage, consider the following discrete

approximation to the Poisson equation:

$$ikE_k = -\sum_j \mathcal{F}(\theta_j, \delta\theta_j), \tag{11}$$

with

$$\mathcal{F} = \frac{1}{2}|f_k(v_j)|e^{i\theta_j}(1 + e^{i\,\delta\theta_j}),$$

where j is the index of discretized velocity $\delta v \equiv v_{j+1} - v_j$ and $\delta\theta_j \equiv \theta_{j+1} - \theta_j$. Since phase mixing is the critical element in determining the amplitude of $|E_k|$, we can formulate the problem in terms of the probability distribution function (pdf) $P(\delta\theta_j)$ of phase differences $\delta\theta_j$. From Fig. 3, we know that θ_j is getting smoothed with time in velocity space. This means that we can approximate this process at the lowest order in terms of diffusion of the pdf, i.e.,

$$\frac{\partial P(\delta\theta_j)}{\partial t} = D_{st}\frac{\partial^2}{\partial\,\delta\theta^2}P, \tag{12}$$

where D_{st} is a phenomenological phase diffusion coefficient. Note that in order to derive the temporal scaling of $|E_k|$, we do not need the detailed form of D_{st}. Equation (12) has the well known solution,

$$P(\delta\theta_j, t) = \frac{1}{\sqrt{2\pi\,\delta\theta_c^2 t}}\exp\left(-\frac{\delta\theta_j^2}{2\,\delta\theta_c^2 t}\right),$$

where $\delta\theta_c^2$ is the characteristic value of $\delta\theta_j^2$. Because θ_f tends to get synchronized, $\delta\theta_c^2$ tends to be a constant C that is close to zero. For large t, we approximately have: $P \propto t^{-1/2}$. With the invariant measure, Eq. (11) gives

$$ik|E_k| = -\sum_j \int \mathcal{F}(\theta_j, \delta\theta_j)P(\delta\theta_j, t)d\,\delta\theta_j \propto t^{-(1/2)}. \tag{13}$$

Thus, $|E_k|$ has the approximate temporal scaling: $|E_k| \propto t^{-(1/2)}$, which agrees with the numerically observed scaling of $|E_k|$. However, it should be noted that $t^{-\beta}$ is more general than $t^{-0.5}$ as we will show later that the damping in the transition stage depends also on the initial perturbation strength.

We end this subsection with some particular snapshots of $\theta_f(k_1, v)$ shown in Fig. 5. As can be seen in the top plot of Fig. 5, at $t = 10\omega_{pe}^{-1}$, the system is dominated by free streaming, i.e., $\theta_f(k, v) \simeq kvt$. The slight deviation of $\theta_f(k_1, v)$ in the range of $v \simeq \pm(2, 3)$ is due to resonant wave particle interactions, but it is very small before the free streaming. In contrast, at $t = 1000\omega_{pe}^{-1}$, the phase synchronization starts to appear since θ_f tends to be locked in the resonant region. Then, at $t = 2000\omega_{pe}^{-1}$, the phase synchronization becomes more apparent, and it starts to spread in velocity space. During the synchronization spreading, θ_f is organized near the resonant region and disorganized in the rest of velocity space, which forms a *chimera phase pattern* [20] as can be seen in the snapshot at $t = 3000\omega_{pe}^{-1}$. Finally, at $t = 5000\omega_{pe}^{-1}$, the phase synchronization is complete across the velocity space with a phase difference of π between the phase of the fast ($|v| > v_r$) and the slow ($|v| < v_r$) electrons. Note that the natural frequency of the slow (fast) particle is accelerated (decelerated) due to this phase difference of π (the detail is given in Sec. IV B). This way, the time variation of θ_f corresponds to the frequency of the plasma wave everywhere.

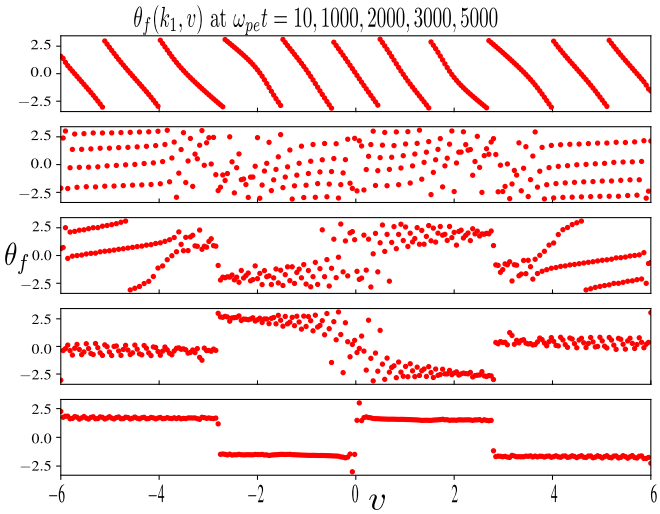

FIG. 5. $\theta_f(k_1, v)$ in velocity space at $\omega_{pe}t = 10$, 1000, 2000, 3000, 5000 (from the top to the bottom).

C. Lifetime of the transition stage

The complete phase synchronization takes a long time as shown in previous simulations. Yet, it would be useful to estimate exactly how long. In order to measure the speed of phase synchronization spreading in velocity space, we define a parameter T_t as the synchronization time, which is the time at which $\theta_f(k_1, v)$ is fully synchronized across the velocity space. Hence, in some sense T_t represents the duration or lifetime of the transition stage. It is observed in numerical simulations that T_t depends on the initial perturbation strength. Figure 6 shows the evolution of $|E(k_1, t)|$ and $\delta\theta_f(k_1, v)$ for a strong (top) and a weak (bottom) initial perturbation where the parameters which define the initial perturbation strengths are $\alpha = 0.5$ and $\alpha = 0.05$, respectively. Although in the case of the strong initial perturbation, the full synchronization in velocity space is observed at $t \simeq 200\omega_{pe}^{-1}$ for the weak initial perturbation, and θ_f is not fully synchronized at the end of the simulation at $t = 10\,000\omega_{pe}^{-1}$.

In order to obtain the relation between T_t and α, we have performed a scan of the parameter $\alpha = [0.5, 0.4, 0.3, 0.2, 0.18, 0.15, 0.13]$, and the full synchronization times that are observed roughly at $T_t = [233, 276, 365, 486, 665, 5000, 9000]\omega_{pe}^{-1}$, respectively, are shown in Fig. 7. The dependence of T_t on α indicates that a strongly (weakly) perturbed system is easier (harder) to be fully synchronized.

We have also checked the behavior of $|R(k_1, v, t)|$ and $|f(k_1, v, t)|$ during these scans, which show that the main reason for the long and slow dampings for the weak initial perturbation case is that the nonlinearity remains too weak to balance free streaming.

Extrapolating from the observed behavior $T_t(\alpha)$, one may argue that T_t will tend to infinity if the initial perturbation is extremely small. This means that the phase mixing as well as the damping of the plasma wave may continue indefinitely or until the wave is completely extinguished. This is a reasonable conclusion also in the sense that if α tends toward zero the system tends to be linear. For example, in the simulation of

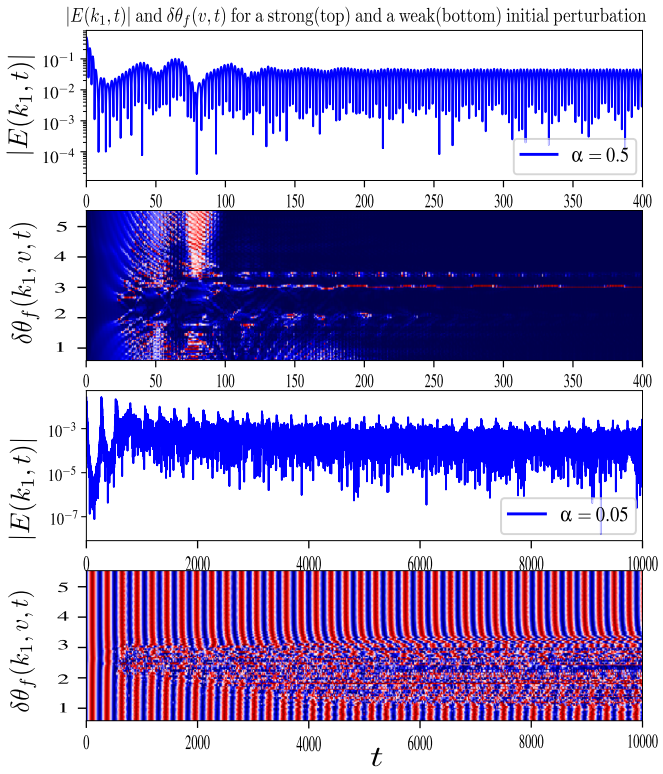

FIG. 6. Comparison of $|E(k_1,t)|$ and $\delta\theta_f(k_1,v,t)$ for a strong (top) and a weak (bottom) initial perturbation. The initial perturbation strengths are $\alpha = 0.5$ and $\alpha = 0.05$, respectively. The color bar is same as that of Fig. 3.

$\alpha = 0.01$, it is hard to observe any significant phase synchronization spreading in velocity space even if the simulation time is long enough.

To summarize, we conclude that both the damping of the form $e^{-\gamma t}$ in linear stage and the damping of the form $t^{-\beta}$ in the transition stage are due to phase mixing of the particle distribution function in velocity space. As a result of the spreading of phase synchronization in velocity space, θ_f tends

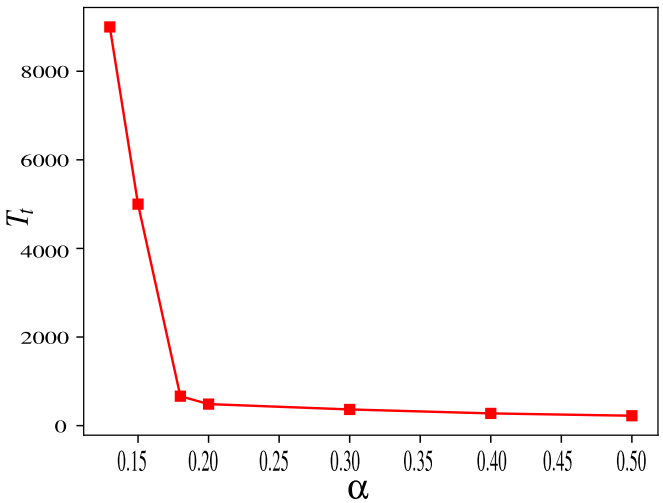

FIG. 7. The lifetime of transition state T_t as a function of the initial perturbation strength α.

to be more organized, and the damping of the plasma wave becomes weaker in the transition stage. When θ_f is fully synchronized in velocity space, the damping is hardly observable, and the system becomes nonlinearly saturated. Since θ_f is organized in the fully nonlinear stage, it is possible to study and understand wave-particle interaction from the perspective of phase evolution.

IV. SELF-REGULATION OF ENERGY TRANSFER IN THE FULLY NONLINEAR STAGE

There are many examples of saturation of the Landau damping in different contexts in plasma physics, such as, for example, the resonance absorption in a laser plasma system [19,29,30] or the current drive theory in Tokamaks [31], etc. Here, we focus on the problem of resonant wave-particle interaction from the perspective of phase dynamics.

In order to do that, we first derive the energy variation as a function of phase and amplitude. The kinetic energy $\mathcal{E}_K$ is defined as: $\mathcal{E}_K(t) \equiv \frac{1}{2}\frac{1}{L_x}\int_x\int_v f(x,v,t)v^2 dv\,dx$ where the distribution function $f(x,v,t)$ can be written using its Fourier transform: $\mathcal{E}_K(t) = \frac{1}{2}\frac{1}{L_x}\int_x\int_v \sum_k f(k,v,t)e^{ikx}v^2 dv\,dx$. Since $\int_0^{L_x} e^{ikx}dx$ gives zero for any nonzero wave number, the kinetic energy becomes: $\mathcal{E}_K(t) = \frac{1}{2}\frac{1}{L_x}\int_v f(k_0,v,t)v^2 dv$. This means that in a periodic system the kinetic energy is stored only in the $k = 0$ mode.

Since $f(k_0,v)$ is the mean value of the electron distribution function, it must be real and non-negative, hence, $\theta(k_0,v)$ as well as $\partial_t\theta(k_0,v)$ should be zero during its evolution, which means

$$\frac{\partial|f(k_0,v)|}{\partial t} = R(k_0,v)\cos[\Theta(k_0,v)],$$
$$\frac{\partial\theta(k_0,v)}{\partial t} = \frac{R(k_0,v)}{|f(k_0,v)|}\sin[\Theta(k_0,v)] = 0, \qquad (14)$$

where $\Theta(k_0,v)$ is either 0 or π. As $\partial_t|f(k_0,v)|$ depends on $\cos[\Theta(k_0,v)]$, $\Theta(k_0,v) = 0\ (\pi)$ means the accumulation (loss) of electrons of velocity v. Using the definition of $\partial_t|f(k_0,v)|$ in Eq. (15), the kinetic energy evolves as $\partial_t\mathcal{E}_K = \frac{1}{2}\frac{1}{L_x}\int_v \mathcal{R}(k_0,v)v^2 dv$. Furthermore, $\mathcal{R}(k_0,v)$ can be rewritten as a convolution in wave number space as follows:

$$\mathcal{R}(k_0,v) = \frac{1}{2}\sum_k\left(E(k)\frac{\partial f^*(k,v)}{\partial v} + E^*(k)\frac{\partial f(k,v)}{\partial v}\right), \qquad (15)$$

integrating $\frac{\partial f(k,v)}{\partial v}$ by part and using $f(k, v = \pm\infty) = 0$, yields

$$\frac{\partial\mathcal{E}_K}{\partial t} = -\frac{1}{L_x}\sum_k\int_v v|E_k||f_k|\cos(\theta_E - \theta_f)dv. \qquad (16)$$

The electric field energy $\mathcal{E}_E$ in wave number space is defined as $\mathcal{E}_E = \frac{1}{2}\frac{1}{L_x}\sum_k|E(k)|^2$. Using $\partial_t|E(k)|$ in Eq. (8), it evolves as

$$\frac{\partial\mathcal{E}_E}{\partial t} = \frac{1}{L_x}\sum_k\int_v v|E_k||f_k|\cos(\theta_E - \theta_f)dv. \qquad (17)$$

Equations (16) and (17) indicate that the total energy of the system should be conserved. Furthermore, the energy flow

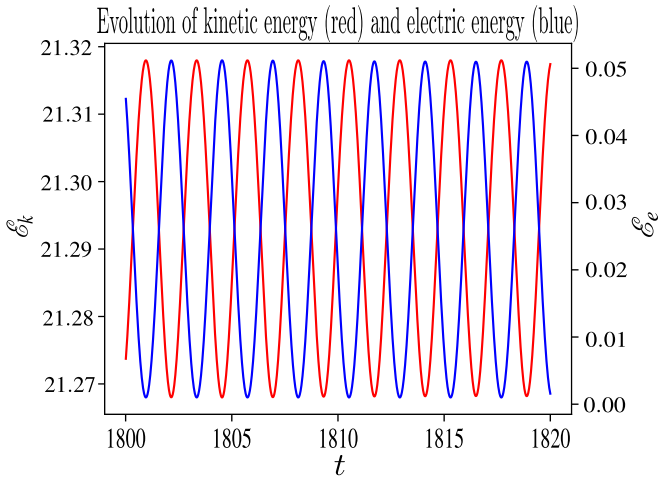

FIG. 8. Evolution of the kinetic energy $\mathcal{E}_K$ (red line) and the electric energy $\mathcal{E}_E$ (shown by the blue line) for $t = [1800\omega_{pe}^{-1}, 1820\omega_{pe}^{-1}]$.

between the wave and the electrons is controlled by the phase difference between the plasma wave and the electron distribution function.

The evolution of the kinetic energy (red) and the electric field energy (blue) in the saturated state are presented in Fig. 8 for the simulation of $\alpha = 0.5$. It shows that the energy conservation is satisfied by the numerical simulation. The kinetic energy is much higher than the electric field energy (or wave energy) because in simulations the particle distribution function has an unperturbed part, which carries a lot of energy but does not participate in the wave-particle energy exchange.

The distribution function during the plasma oscillation is shown on the (x, v) plane in Fig. 9. The left and the right figures present $f(x, v)$ at the moment where the wave energy is maximum and minimum, respectively. The holes are formed due to the trapping of resonant electrons in the electric potential well [9], which propagate in different directions along the x axis with the velocity equal to the phase velocity of the wave. During the propagation of these phase holes, $f(x, v)$ is perturbed along the v direction, which leads to the appearance of energy fluctuations.

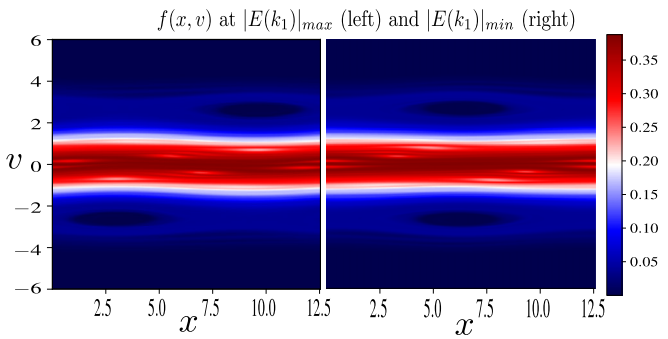

FIG. 9. The electron distribution function $f(x, v)$ in phase space at the maximum (left) and the minimum (right) of $|E(k_1)|$.

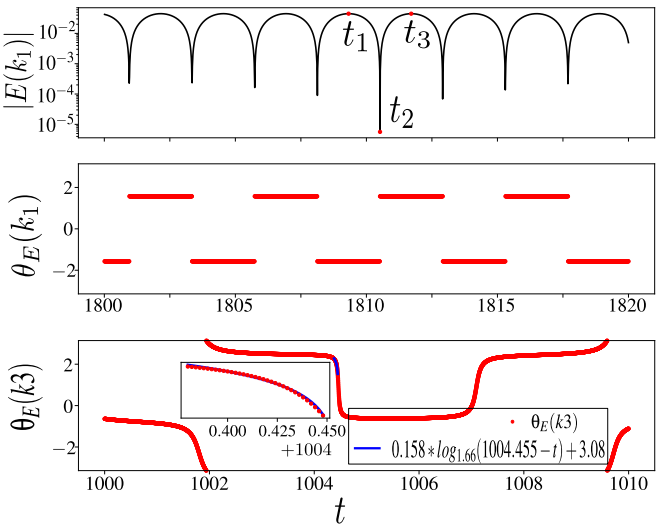

FIG. 10. Evolution of $|E(k_1)|$ (top) and $\theta_E(k_1)$ (center) at $t = [1800, 1820]$. The bottom figure presents the detailed evolution of $\theta_E(k_3)$ (bottom) near the phase jump, and a logarithmic function of t (blue) is used to fit $\theta_E(k_3)$ during the phase jump. Recall that $k_n = \frac{2\pi n}{L_x}$.

A. $\mathcal{E}_E \to \mathcal{E}_K$, determined by θ_E

The energy transfer from the plasma wave to the electrons is determined by the sign of θ_E. This can be seen from Fig. 10, which shows the detailed evolution of $|E(k_1)|$ and $\theta_E(k_1)$ in the saturated state, where t_1 and t_2 correspond to the moments where $|E(k_1)|$'s are maximum and minimum, respectively, and t_3 is the moment when $|E(k_1)|$ is maximum in the next period. During the oscillation of k_1 mode, the maximum of $|E(k_1)|$ is constant [i.e., $|E(k_1, t_1)| \approx |E(k_1, t_3)|$] whereas its minimum tends to zero. Detailed analysis of the numerical simulation with a very small integration time step near its minimum shows that whereas the minimum of $|E(k_1)|$ approaches zero, it does not exactly become zero because $|E(k_1)|$ changes instantaneously from decreasing regime to increasing regime as it approaches zero. This happens because of the instantaneous phase jump by π of $\theta_E(k_1)$.

In Fig. 10, it is observed that $\theta_E(k_1)$ is fixed at $\frac{\pi}{2}$ (or $-\frac{\pi}{2}$) during one period, which means that $\partial_t \theta_E$ is zero. The behavior of $\theta_E(k_1)$ is determined by Eq. (9), which can be rewritten as

$$\frac{\partial \theta_E(k)}{\partial t} = \frac{1}{|E(k)|} \int_{-\infty}^{+\infty} v|f(k)| \Big[\sin[\theta_f(k)]\cos[\theta_E(k)] + \cos[\theta_f(k)]\sin(\theta_E(k)] \Big] dv. \tag{18}$$

Since θ_E is $\pm\frac{\pi}{2}$ during one period, the first term in Eq. (18) vanishes. The second term vanishes too due to the structure of the distribution function in velocity space. We can see this by writing the Poisson equation in the same expanded form of (18) as

$$ik|E|[\cos(\theta_E) + i\sin(\theta_E)] = -\int |f|[\cos(\theta_f) + i\sin(\theta_f)]dv.$$

Because $\theta_E(k_1) = \pm\frac{\pi}{2}$, the imaginary part of the Poisson equation should be zero, [i.e., $i\int |f_k|\sin(\theta_f)dv = 0$], and in order to satisfy this θ_f should be an odd function of v,

$$\theta_f(k_1, v) = -\theta_f(k_1, -v),$$
$$|f(k_1, v)| = |f(k_1, -v)|.$$

Using these relations, the second term of Eq. (18), i.e., $\int_{-\infty}^{+\infty} v|f(k_1, v)|\cos[\theta_f(k_1, v)]dv$ should be zero. As a result of this, $\theta_E(k_1)$ can remain fixed at $\pm\frac{\pi}{2}$ during one period.

In Eq. (18), $|E(k)|$ is the denominator in the evolution of $\theta_E(k)$. This produces a singularity for $\theta_E(k)$ once $|E(k)|$ becomes extremely small [32]. The jump of $\theta_E(k)$ results from this singularity. The detailed structure of $\theta_E(k_3)$ (red) near the phase jump is shown in the bottom plot of Fig. 10, and it can be fit with a logarithmic function (blue). Note that we present the result of the third harmonic, i.e., k_3 mode rather than the k_1 mode in order to show that the phase jump is a general feature of all the Fourier modes k. When $|E(k)|$ is minimum near t_2, θ_E diverges, and one may assume: $|\partial_t \ln\theta_E| \gg |\partial_t \ln|E||$. Therefore, $|E(k)|$ as well as its temporal variation can be seen as a constant compared to the rapid variation of $\theta_E(k)$ near t_2. With this assumption, one has $|E(k)| \simeq c_0 + c_1 t$, where c_0 and c_1 present $|E(k)|$ and the integral of $\partial_t|E(k)|$ at a certain moment t near t_2. This yields: $\partial_t\theta_E \propto \frac{1}{|E|} \propto \frac{1}{t_c - t}$ with $t_c \equiv c_0/c_1$, the time where the jump of $\theta_E(k)$ occurs. Thus, $\theta_E(k)$ has a logarithmic finite-time singularity (FTS) at the point where the $|E(k)|$ is minimum: $\theta_E \propto \ln(t_c - t)$. Furthermore, when θ_E leaves one fixed point, it is attracted by another one because the new invariance of θ_E can be built once it is close to the next fixed point. In between t_1 and t_2, the field energy decreases as it is transferred to particles. When it reaches its minimum value at t_2, θ_E jumps instantaneously by π due to the FTS. Since the energy evolves as: $\partial_t\mathcal{E}_E \propto \cos(\theta_E - \theta_f)$, the phase jump of θ_E changes the sign of the energy transfer before and after t_2, that is, $\partial_t\mathcal{E}_E(t_2 + \delta t) \simeq -\partial_t\mathcal{E}_E(t_2 - \delta t)$. This means that after t_2 the kinetic energy will start to be transferred back to the plasma wave when the field energy is at its minimum. This analysis is rigorously true assuming that θ_f cannot jump instantaneously when θ_E jumps by π. The dynamics of θ_f is discussed in the next subsection, and it controls the energy transfer from the electrons to the electric wave.

B. $\mathcal{E}_K \rightarrow \mathcal{E}_E$, controlled by θ_f

In Eq. (6), the evolution of θ_f is determined by a constant natural frequency $-kv$ and Θ. In order to understand the behavior of θ_f, it is necessary to understand the evolution of Θ. The complex order parameter can be represented as a convolution in wave-number space: $\mathcal{R}(k, v) = \sum_p E(p, t)\frac{\partial f(k-p,v)}{\partial v}$. The numerical simulations show that the wave-particle interaction in the nonlinearly saturated state is dominated by the interaction with the background mode $f(k_0)$. Hence, $\mathcal{R}(k_1, v)$ can be estimated by $\mathcal{R}(k_1, v) \cong E(k_1, t)\frac{\partial f(k_0,v)}{\partial v}$, which can then be used to argue $\Theta(k_1, v) \cong \text{sgn}(\frac{\partial f(k_0,v)}{\partial v})\theta_E(k_1)$. In a Maxwellian plasma $\partial_v f(k_0, v > 0)$ is negative, except in the wave-particle resonance region as shown in the top of Fig. 11. So $\Theta(k_1, v > 0)$ equals $-\theta_E(k_1)$ in the nonresonant region. On the other hand, in the wave-particle resonance region

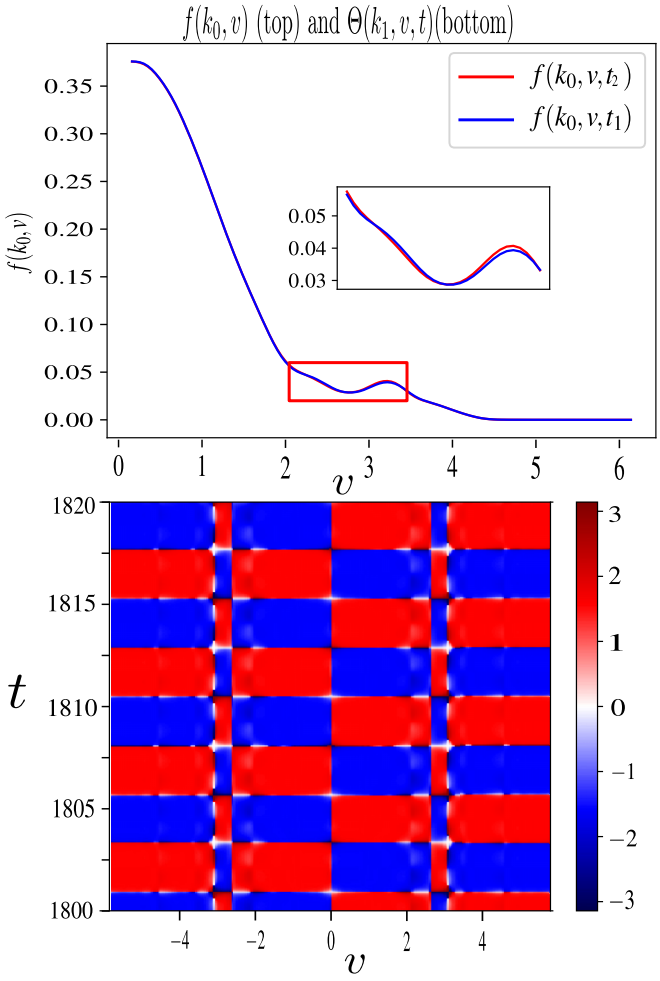

FIG. 11. The top figure shows $f(k_0, v)$ at t_1 (blue) and t_2 (red). The bottom figure shows $\Theta(k_1, v)$ as a function of time t and velocity v.

$\partial_v f(k_0, v \sim v_r)$ is positive and, hence, $\Theta(k_1, v \sim v_r)$ equals $\theta_E(k_1)$. The detailed structure of $\Theta(k_1, v, t)$ is shown in the bottom of Fig. 11. It shows that $\Theta(k_1, v)$ is strongly correlated with $\theta_E(k_1)$. In other words, when $\theta_E(k_1)$ jumps by π, $\Theta(k_1, v)$ also jumps by π, regardless of its detailed velocity space structure.

Since Θ is same for the fast and slow electrons, but a difference of π exists between $\theta_f(k_1, v < v_r)$ and $\theta_f(k_1, v > v_r)$ as shown in Fig. 12. This difference can slow down (accelerate) the natural frequency of the fast (slow) electrons, based on Eq. (6). This allows all the electrons with different natural frequencies to be able to follow the frequency of the plasma wave resulting in full synchronization in the nonlinear saturated state.

Note also that, the energy transfer depends on $\cos(\theta_f - \theta_E)$ with θ_E remaining a constant during one period. A difference of π between the fast and the slow electrons also means that these two parts play opposite roles in energy evolution. The quantitative contribution of these two parts in the energy transfer is presented in the bottom plot of Fig. 12, where c_H and c_L, respectively, are defined as $c_H \equiv \int_{v>v_r} v|f(k_1)|\cos(\theta_f - \theta_E)dv$ and $c_L \equiv \int_{0<v<v_r} v|f(k_1)|\cos(\theta_f - \theta_E)dv$. It shows

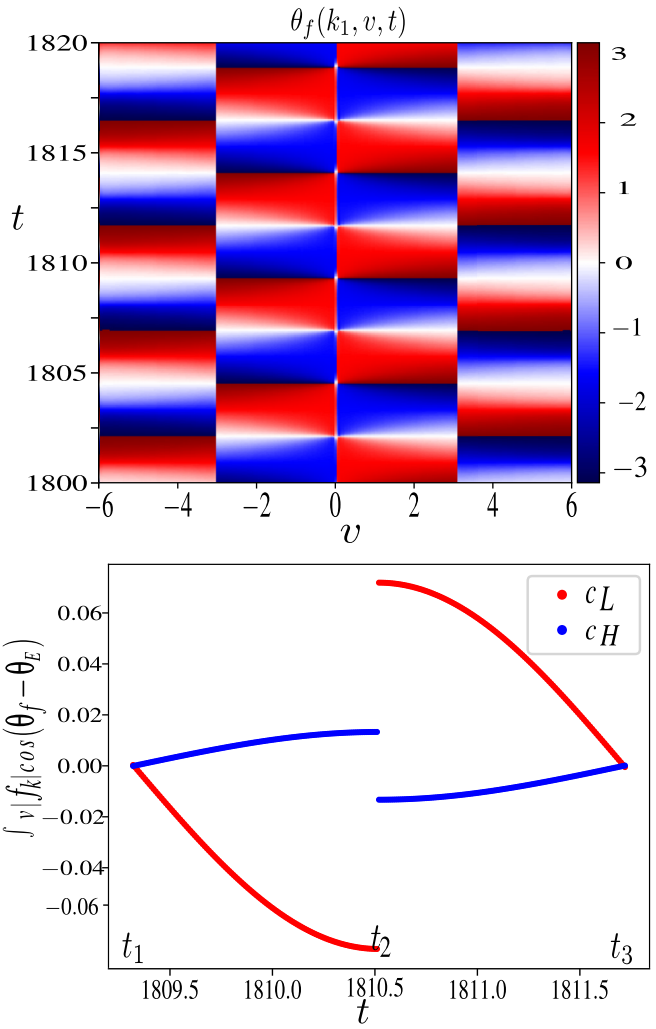

FIG. 12. The top figure presents the structure of $\theta_f(k_1)$ in velocity space as a function of time. The bottom figure presents the quantitative contribution of the high velocity zone c_H and low velocity zone c_L to $|E(k_1)|$ during one oscillation.

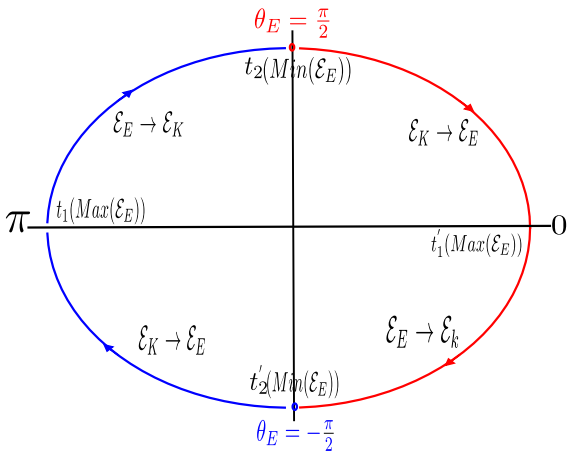

FIG. 13. Evolution of $\theta_f(k_1, 0 < v < v_r)$. The blue (red) line is the trajectory of $\theta_f(k_1, 0 < v < v_r)$ during the period of $\theta_E = -\frac{\pi}{2}(\frac{\pi}{2})$. $\theta_f(k_1, v > v_r)$ has a difference of π compared to $\theta_f(k_1, 0 < v < v_r)$ and $\theta_f(-v) = -\theta_f(v)$.

that the evolution of $|E(k_1)|$ is dominated by the slow electrons. This is due to the fact that $|f(k_1, |v| > v_r)|$ is much smaller compared to $|f(k_1, |v| < v_r)|$ in a Maxwellian plasma.

Figure 12 also shows that $\theta_f(k_1, v > 0)$ rotates continuously in the clockwise direction, and, thus, $\partial_t \theta_f(k_1, v > 0)$ is always negative. As $\theta_E = \pm\frac{\pi}{2}$, the Poisson equation becomes: $k|E|\sin(\theta_E) = 2\int_{v>0} |f|\cos(\theta_f)dv$. From this relation one may induce that when θ_E is $\frac{\pi}{2}$ $(-\frac{\pi}{2})$, the phase of the dominant part, i.e., $\theta_f(k_1, 0 < v < v_r)$, should be in the range of $(-\frac{\pi}{2}, \frac{\pi}{2})$ $[(\frac{\pi}{2}, \frac{3\pi}{2})]$. Meanwhile $\Theta(v > 0)$ remains fixed at $-\frac{\pi}{2}$ $(\frac{\pi}{2})$, hence, $\sin[\Theta - \theta_f(k_1, 0 < v < v_r)]$ is negative. Therefore, $\partial_t \theta_f(k_1, v < v_r)$ is always negative during the evolution of the system. In the high velocity zone, $\partial_t \theta_f(k_1, v > v_r)$ is negative because the free streaming frequency is very large.

Since θ_E is constant during one period and θ_f rotates continuously on the complex plane, once θ_f passes a certain threshold, the sign of $\cos(\theta_E - \theta_f)$ changes, resulting in the inversion of energy transfer. In other words, when θ_E takes the value of $\frac{\pi}{2}$ in one period, $\theta_f(k_1, 0 < v < v_r)$ moves from $\frac{\pi}{2}$ to $-\frac{\pi}{2}$. In this case $\theta_f(k_1, 0 < v < v_r) = 0$ is the threshold of the energy transfer. When $\theta_f(k_1, 0 < v < v_r)$ is localized in the interval $(\frac{\pi}{2}, 0)$, $\partial_t \mathcal{E}_E \propto \cos(\theta_E - \theta_f)$ is positive, and the kinetic energy is transferred to the field. When $\theta_f(k_1, v < v_r)$ passes this threshold and moves into the interval $(0, -\frac{\pi}{2})$, the field energy is transferred back to the electrons. In the case of $\theta_E = -\frac{\pi}{2}$, π is the threshold of $\theta_f(v < v_r)$. From the Poisson equation, one may find that when $|E_k|$ is maximum (minimum), θ_f should be 0 and π $(\pm\frac{\pi}{2})$. So the transfer of kinetic energy to field energy is reversed at the maximum of $|E_k|$.

The rotation of $\theta_f(k_1, 0 < v < v_r)$ on the complex plane, and the energy transfer during the evolution of θ_f is summarized in Fig. 13. If $\theta_{f,E}(v < v_r)$ is localized in $(0, \frac{\pi}{2})$, the kinetic energy will be transferred to the electric field. This transfer is limited when θ_f passes its threshold (0 or π). If $\theta_{f,E}(v < v_r)$ is localized in $(\frac{\pi}{2}, \pi)$, the wave energy will now transfer to the electrons. And this transfer is stopped by the instantaneous phase jump of θ_E due to the finite time singularity. Thus, the system evolves self-consistently.

V. CONCLUSION

In this paper, we have studied the transition from linear Landau damping to the nonlinear BGK mode from the perspective of phase dynamics. We proposed a formulation of treating the nonlinear wave-particle interaction term playing the role of a complex order parameter, which allowed us to deepen our understanding of the nonlinear wave-particle interaction as a process of phase synchronization.

As a result of detailed analysis of numerical simulations of the evolution of initial perturbations in a one dimensional Vlasov-Poisson system, we found that the phase synchronization appears initially in the wave-particle resonant region and then spreads to the rest of the velocity space through a

process that we call *phase synchronization spreading*. As this happens, the phase mixing becomes weaker and weaker, and the plasma wave transitions from the usual exponential form of linear Landau damping to an algebraic damping of the form $t^{-\beta}$. This damping can persist indefinitely if the initial perturbation is sufficiently small.

We have also shown that the phase mixing provides a positive feedback mechanism for the nonlinear phase coupling by decreasing the amplitude of the electron distribution function. This means that unless the amplitudes become negligibly small, the tendency for phase locking keeps growing in competition with the constant free streaming that leads to phase slipping. This results, eventually, in a fully synchronized state.

Although the usual phenomenon of forward or inverse Landau damping can explain how individual particles can accelerate and decelerate depending on if they are faster or slower than the wave, it is the collective indirect coupling among individual electrons as they accelerate and decelerate because of their nonlinear interaction with the wave that results in synchronization. This means that the underlying physical mechanism of phase synchronization can be identified as occurring through the synchronization of individual electron motions as they accelerate or decelerate due to nonlinear wave-particle interaction, somewhat similar to the synchronization of other weakly coupled oscillator systems.

Note also that in a fully synchronized state, the phase evolution of individual electrons matches the frequency of the plasma wave, and the energy is able to be transferred back and forth between the wave and the electrons in a periodic fashion. This energy transfer is self-regulated by the phases of the plasma wave and the electron distribution function, where θ_E is constant during one period and θ_f evolves continuously in a self-consistent manner. In particular, θ_E jumps instantaneously by π when the wave energy is at its minimum, resulting in energy transfer from the electrons to the wave. On the other hand, when the wave energy is at its maximum, θ_f arrives at its threshold value, which causes the wave energy to be transferred back to the electrons.

The method that we have developed in this paper may be applied to more complex systems, such as the Gyrokinetic Vlasov-Poisson system or its electromagnetic generalization [33], which may provide a better understanding of the nonlinear evolution of fusion plasmas. It may also be applied to other systems where 1D Vlasov-Poisson can be applicable, such as, for example, the description of self-gravitating matter in cosmological systems [34,35].

[1] L. Landau, J. Phys. USSR **10**, 25 (1946).
[2] J. H. Malmberg and C. B. Wharton, Phys. Rev. Lett. **13**, 184 (1964).
[3] C. W. Myung, I. H. Won, H. Y. Kim, J.-S. Lee, G. S. Yun, and J. K. Lee, J. Phys. Soc. Jpn. **83**, 074502 (2014).
[4] J. T. Parker and P. J. Dellar, J. Plasma Phys. **81**, 305810203 (2015).
[5] C. Cheng and G. Knorr, J. Comput. Phys. **22**, 330 (1976).
[6] S. H. Strogatz, R. E. Mirollo, and P. C. Matthews, Phys. Rev. Lett. **68**, 2730 (1992).
[7] C. Mouhot and C. Villani, J. Math. Phys. **51**, 015204 (2010).
[8] B. B. Kadomtsev, Sov. Phys. Usp. **11**, 328 (1968).
[9] P. H. Diamond, S.-I. Itoh, and K. Itoh, *Modern Plasma Physics* (Cambridge University Press, Cambridge, U.K. 2010).
[10] M. Lesur, P. H. Diamond, and Y. Kosuga, Plasma Phys. Controlled Fusion **56**, 075005 (2014).
[11] I. B. Bernstein, J. M. Greene, and M. D. Kruskal, Phys. Rev. **108**, 546 (1957).
[12] M. B. Isichenko, Phys. Rev. Lett. **78**, 2369 (1997).
[13] G. Manfredi, Phys. Rev. Lett. **79**, 2815 (1997).
[14] T. O'Neil, Phys. Fluids **8**, 2255 (1965).
[15] D. Bénisti, D. J. Strozzi, L. Gremillet, and O. Morice, Phys. Rev. Lett. **103**, 155002 (2009).
[16] C. Villani, Phys. Plasmas **21**, 030901 (2014).
[17] A. Pikovsky, M. G. Rosenblum, and J. Kurths, *Synchronization, A Universal Concept in Nonlinear Sciences* (Cambridge University Press, Cambridge, UK, 2001).
[18] F. Amiranoff, C. Riconda, M. Chiaramello, L. Lancia, J.-R. Marqués, and S. Weber, Phys. Plasmas **25**, 013114 (2018).
[19] M. S. Hur, R. R. Lindberg, A. E. Charman, J. S. Wurtele, and H. Suk, Phys. Rev. Lett. **95**, 115003 (2005).
[20] D. M. Abrams and S. H. Strogatz, Phys. Rev. Lett. **93**, 174102 (2004).
[21] Y. Kuramoto, *Chemical Oscillations, Waves, and Turbulence* (Springer-Verlag, New York, 1984).
[22] S. H. Strogatz, Physica D **143**, 1 (2000).
[23] S. Moradi, J. Anderson, and O. D. Gürcan, Phys. Rev. E **92**, 062930 (2015).
[24] R. Adler, Proc. IEEE **61**, 1380 (1946).
[25] B. D. Fried and S. D. Conte, *The Plasma Dispersion Function* (Academic, New York, 1961).
[26] N. V. Kampen, Physica **21**, 949 (1955).
[27] Z. B. Guo and P. H. Diamond, Phys. Rev. Lett. **114**, 145002 (2015).
[28] T. Utsumi, T. Kunugi, and J. Koga, Comput. Phys. Commun. **108**, 159 (1998).
[29] A. Bergmann, S. Hüller, P. Mulser, and H. Schnabl, Europhys. Lett. **14**, 661 (1991).
[30] A. Bergmann and P. Mulser, Phys. Rev. E **47**, 3585 (1993).
[31] N. J. Fisch, Rev. Mod. Phys. **59**, 175 (1987).
[32] Z. B. Guo, Y. H. Wang, and S. K. Xu, Phys. Rev. E **101**, 030201(R) (2020).
[33] T. S. Hahm, Phys. Fluids **31**, 2670 (1988).
[34] D. Lynden-Bell, Mon. Not. R. Astron. Soc. **136**, 101 (1967).
[35] S. Colombi and J. Touma, Mon. Not. R. Astron. Soc. **441**, 2414 (2014).